

## Nonlinear polarization rotation of a Gaussian pulse propagating through an EIT medium

This content has been downloaded from IOPscience. Please scroll down to see the full text.

2014 J. Phys. B: At. Mol. Opt. Phys. 47 045503

(<http://iopscience.iop.org/0953-4075/47/4/045503>)

View [the table of contents for this issue](#), or go to the [journal homepage](#) for more

Download details:

IP Address: 147.91.1.43

This content was downloaded on 04/04/2016 at 14:16

Please note that [terms and conditions apply](#).

# Nonlinear polarization rotation of a Gaussian pulse propagating through an EIT medium

J Dimitrijević, D Arsenović and B M Jelenković

Institute of Physics, University of Belgrade, Pregrevica 118, 10080 Belgrade, Serbia

E-mail: [jelena.dimitrijevic@ipb.ac.rs](mailto:jelena.dimitrijevic@ipb.ac.rs)

Received 26 September 2013, revised 19 December 2013

Accepted for publication 30 December 2013

Published 4 February 2014

## Abstract

We study numerically the nonlinear magneto-optical rotation of polarization (NMOR) of the laser pulse during its propagation through a cold Rb cloud with induced Zeeman coherences and electromagnetically induced transparency. Evolution of NMOR is calculated by solving the Maxwell–Bloch equations. We consider a linearly polarized Gaussian pulse with different pulse peak amplitudes and widths. For an intensity peak of  $5 \text{ mW cm}^{-2}$  and full-width at half-maximum of  $10 \mu\text{s}$ , transient behaviour of NMOR does not follow the pulse intensity variation: NMOR begins to decrease as the pulse's intensity nears its peak value. When the pulse has a smaller peak intensity, NMOR behaves qualitatively differently: the angle of rotation constantly increases during the pulse propagation. Observed differences are explained by the optical pumping into the dark state and the behaviour of the ground-state coherences subjected to coherent population trapping. The same pulse intensity, from different sides of the pulse, during rising and falling sides, produces qualitatively different NMOR shapes, its amplitudes and widths which result can be explained by the successive excitation of atoms during the pulse propagation. It was shown that increasing the relaxation rates of the ground-state coherences, shifts the maximum of the NMOR to higher magnetic field, while the atomic density strongly influences the magnitude of the NMOR.

Keywords: magneto-optical effects, electromagnetically induced transparency, electromagnetic pulses, light propagation

(Some figures may appear in colour only in the online journal)

## 1. Introduction

Rotation of the polarization plane of light travelling through an atomic vapour, subjected to magnetic field, has been studied for more than a century. The main characteristic of the linear resonant Faraday effect is that, for Larmor frequencies smaller than the resonance line width, the magnitude of the rotation is proportional to a magnetic field. For nonlinear magneto-optical rotation (NMOR) [1, 2], nonlinear contributions appear in characteristic, dispersively shaped dependence on the magnetic field.

The origin of magneto-optical rotation lies in the fact that the medium behaves differently for the two components of the field, displaying what is known as circular birefringence

or linear dichroism. The magnetic field, when applied to an initially isotropic medium, creates asymmetry between medium susceptibilities, corresponding to two circularly polarized components of the field. Asymmetry can happen when the magnetic field is longitudinal with respect to light propagation (Faraday effect, causing circular birefringence) or is transverse to  $\vec{k}$  (Voigt effect, causing linear dichroism). Resultant circular birefringence and linear dichroism induce magneto-optical rotation, i.e. the polarization plane of the light emerging out of the medium is rotated with respect to that of the incident.

It is however interesting to relate NMOR to the combined effects of the laser field and the magnetic field in the context of coherent control of the polarization rotation [3–5]. Namely,

NMOR is associated with the light-generated redistribution of populations by optical pumping, and also by the creation of coherences between magnetic sublevels of atomic or molecular ground and/or excited states. This makes NMOR closely related to other coherence effects, like electromagnetically induced transparency (EIT) [6, 7], coherence population trapping (CPT) [8, 9] and the slow propagation of light [10, 11].

NMOR is typically studied as a function of light detuning from atomic resonance, in the presence of the constant magnetic field or as a function of the magnetic field for the light tuned to the resonance. When both laser field and the external magnetic field are present, transmission line shapes show interplay between two fields resulting with suppressed and enhanced rotation signals. Also, NMOR is typically studied for the continuous-wave fields when it is of interest to know the amount of rotation in the steady state. However, in the case of amplitude modulated electromagnetic field propagating through the resonant gaseous media, the presence of magnetic field leads to time-dependent magneto-optical rotation.

Interest in laser pulse NMOR is focused on achieving a better understanding of the relation between polarization of the medium during the pulse propagation, and the subsequent effects on the polarization of the light pulse. Investigation of pulse NMOR behaviour is then directly related to studies of pulse propagation through atomic medium [11], slow and stored light [12, 13] and optical switching [14]. The NMOR of pulsed light has been analysed in the context of slow light [15–17]. Budker *et al* [15] demonstrated the relation between the reduced light group velocity and nonlinear magneto-optics. It was shown that the time-dependent optical rotation can mask the storage of light signal [16]. Ruseckas *et al* [17] have shown that the orbital angular momentum of slow light manifests in a rotation of the polarization plane of linearly polarized light.

In this paper we study theoretically the transient NMOR behaviour of the light pulse propagating through the atomic medium in the presence of longitudinal magnetic field. Frequency of the linearly polarized light is tuned to the  $F_g = 2 \rightarrow F_e = 1$  hyperfine transition in the Rb, D1 line. Therefore, the pulse is inducing EIT in the atomic medium as it propagates. The properties of NMOR are obtained by solving density matrix equations for the atomic coherences and populations along with the Maxwell equations describing pulse propagation of the electromagnetic field through the cold gas. We assume the Gaussian shape for the light pulse and perform calculations for different pulse amplitudes and widths. Transient behaviour of NMOR is compared to that of ground-state coherences subjected to CPT, and their relation is discussed. Influence of ground-states relaxation and atomic density on the magnetic field dependence of rotation angle, as the pulse propagates through the atomic medium, is presented.

## 2. Theoretical model

We solve the Maxwell–Bloch equations for the  $F_g = 2 \rightarrow F_e = 1$  transition (see figure 1) in the  $^{87}\text{Rb}$ , D1 line, for different longitudinal magnetic fields. Evolution of the density matrix  $\hat{\rho}(t, z)$  is obtained from the optical-Bloch equations:

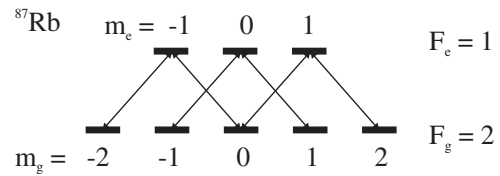


**Figure 1.**  $F_g = 2$  and  $F_e = 1$  hyperfine levels with the notation of magnetic sublevels.

$$\frac{d\hat{\rho}(t, z)}{dt} = -\frac{i}{\hbar}[\hat{H}_0, \hat{\rho}(t, z)] - \frac{i}{\hbar}[\hat{H}_I, \hat{\rho}(t, z)] - \hat{S}\hat{E}\hat{\rho}(t, z) - \gamma\hat{\rho}(t, z) + \gamma\hat{\rho}_0. \quad (1)$$

From equation (1) we calculate the evolution of the density matrix  $\hat{\rho}$ . Indexes  $g$  and  $e$  stand for the ground and excited levels, respectively. The diagonal elements of the density matrix,  $\rho_{g_i, g_i}$  and  $\rho_{e_i, e_i}$  are the populations, while elements  $\rho_{g_i, g_j}$  and  $\rho_{e_i, e_j}$  are Zeeman coherences, and  $\rho_{g_i, e_j}$  and  $\rho_{e_i, g_j}$  are optical coherences. The usual substitution for optical coherences has been introduced:

$$\begin{aligned} \rho_{g_i, e_j} &= e^{i\omega t - ikz} \tilde{\rho}_{g_i, e_j}, \\ \rho_{e_i, g_j} &= e^{-i\omega t + ikz} \tilde{\rho}_{e_i, g_j}. \end{aligned} \quad (2)$$

In equation (1),  $\hat{H}_0$  describes the interaction of Rb atoms with magnetic field  $\vec{B}$ . The direction of the magnetic field is also the direction of the pulse propagation and is taken to be the quantization axis. Magnetic sublevels are split due to the Zeeman effect by  $E_{g(e)} = \mu_B l_{F_{g(e)}} m_{g(e)} B$ , where  $m_{g(e)}$  are magnetic quantum numbers of the ground and excited levels,  $\mu_B$  is the Bohr magneton and  $l_{F_{g,e}}$  is the Lande gyromagnetic factor for the hyperfine level. The interaction of atoms with electromagnetic pulse, with electric field vector  $\vec{E}(t, z)$ , is given with Hamiltonian  $\hat{H}_I$ .  $\hat{S}\hat{E}$  is the spontaneous emission operator with the rate  $\Gamma$ . Due to a finite time that an atom spends in the laser beam, all density matrix elements are relaxing with the same rate  $\gamma$ . The term  $\gamma\hat{\rho}_0$  describes the continuous flux of atoms entering the laser beam, where we take equal population of the ground Zeeman sublevels for these atoms. The role of the laser detuning is not discussed.

The electric field vector is

$$\begin{aligned} \vec{E}(t, z) &= \vec{e}_x E_x(t, z) \cos(\omega t - kz + \varphi_x(t, z)) \\ &+ \vec{e}_y E_y(t, z) \cos(\omega t - kz + \varphi_y(t, z)), \end{aligned} \quad (3)$$

where  $\omega > 0$  is the laser angular frequency,  $\omega = \pm ck$ ,  $\vec{k}$  is the wave vector (we take  $k > 0$  for the propagation towards the positive direction of the  $z$ -axis) and  $c$  is the speed of light.  $E_x(t, z)$  and  $E_y(t, z)$  are real Cartesian components of the electric field amplitude, while real quantities  $\varphi_x(t, z)$  and  $\varphi_y(t, z)$  are associated phases. In the following text we omit dependence of all quantities on  $t$  and  $z$ .

The angle of rotation  $\phi$  is introduced here, when Cartesian unit vectors are rotated like

$$\vec{e}_x \rightarrow \vec{e}_x \cos \phi + \vec{e}_y \sin \phi, \quad \vec{e}_y \rightarrow \vec{e}_y \cos \phi - \vec{e}_x \sin \phi. \quad (4)$$

The electric field vector  $\vec{E}$ , when cosine functions in equation (3) are written in exponential form, is

$$\begin{aligned} \vec{E} = & \frac{1}{2}E_x(\vec{e}_x \cos \phi + \vec{e}_y \sin \phi)e^{i\omega t - ikz + i\varphi_x} \\ & + \frac{1}{2}E_x(\vec{e}_x \cos \phi + \vec{e}_y \sin \phi)e^{-i\omega t + ikz - i\varphi_x} \\ & + \frac{1}{2}E_y(\vec{e}_y \cos \phi - \vec{e}_x \sin \phi)e^{i\omega t - ikz + i\varphi_y} \\ & + \frac{1}{2}E_y(\vec{e}_y \cos \phi - \vec{e}_x \sin \phi)e^{-i\omega t + ikz - i\varphi_y}. \end{aligned} \quad (5)$$

After we make transformation to the complex spherical unit vectors basis:

$$\vec{e}_x = \frac{\vec{\sigma}^- - \vec{\sigma}^+}{\sqrt{2}}, \quad \vec{e}_y = \frac{i(\vec{\sigma}^- + \vec{\sigma}^+)}{\sqrt{2}}, \quad \vec{e}_z = \vec{\sigma}^0, \quad (6)$$

the electric field vector is given in terms of complex amplitudes,  $E_{++}$ ,  $E_{+-}$ ,  $E_{-+}$  and  $E_{--}$  as

$$\begin{aligned} \vec{E} = & e^{i\omega t - ikz}(\vec{\sigma}^- E_{-+} + \vec{\sigma}^+ E_{++}) \\ & + e^{-i\omega t + ikz}(\vec{\sigma}^- E_{--} + \vec{\sigma}^+ E_{+-}). \end{aligned} \quad (7)$$

In equation (7) the following substitution has been made:

$$\begin{aligned} E_{+-} = & \frac{e^{-i\phi}}{2\sqrt{2}}(-E_x e^{-i\varphi_x} + iE_y e^{-i\varphi_y}), \\ E_{--} = & \frac{e^{i\phi}}{2\sqrt{2}}(E_x e^{-i\varphi_x} + iE_y e^{-i\varphi_y}), \\ E_{++} = & \frac{e^{-i\phi}}{2\sqrt{2}}(-E_x e^{i\varphi_x} + iE_y e^{i\varphi_y}), \\ E_{-+} = & \frac{e^{i\phi}}{2\sqrt{2}}(E_x e^{i\varphi_x} + iE_y e^{i\varphi_y}). \end{aligned} \quad (8)$$

From equation (8) we see that complex amplitudes of electric field are not mutually independent i.e.  $(E_{++})^* = -E_{--}$  and  $(E_{+-})^* = -E_{-+}$ .

Maxwell-Bloch equations representing equations of motion for the complex amplitudes  $E_{++}$ ,  $E_{+-}$ ,  $E_{-+}$  and  $E_{--}$  (given in equation (8)) are solved for the propagation along the  $z$ -axis:

$$\begin{aligned} \left(\frac{\partial}{\partial z} + \frac{1}{c} \frac{\partial}{\partial t}\right) E_{+-} = & + i \frac{kN_c}{2\epsilon_0} P_{+-}, \\ \left(\frac{\partial}{\partial z} + \frac{1}{c} \frac{\partial}{\partial t}\right) E_{--} = & + i \frac{kN_c}{2\epsilon_0} P_{--}, \\ \left(\frac{\partial}{\partial z} + \frac{1}{c} \frac{\partial}{\partial t}\right) E_{++} = & - i \frac{kN_c}{2\epsilon_0} P_{++}, \\ \left(\frac{\partial}{\partial z} + \frac{1}{c} \frac{\partial}{\partial t}\right) E_{-+} = & - i \frac{kN_c}{2\epsilon_0} P_{-+}. \end{aligned} \quad (9)$$

In equation (9) we introduced the following quantities:

$$\begin{aligned} P_{+-} = & - \sum_{e_i \leftrightarrow g_j} \tilde{\rho}_{e_i, g_j} \mu_{g_j, e_i, -1}, \\ P_{--} = & - \sum_{e_i \leftrightarrow g_j} \tilde{\rho}_{e_i, g_j} \mu_{g_j, e_i, +1}, \\ P_{++} = & - \sum_{g_i \leftrightarrow e_j} \tilde{\rho}_{g_i, e_j} \mu_{e_j, g_i, -1}, \\ P_{-+} = & - \sum_{g_i \leftrightarrow e_j} \tilde{\rho}_{g_i, e_j} \mu_{e_j, g_i, +1}, \end{aligned} \quad (10)$$

where summation is taken over dipole-allowed transitions induced by the laser. These four variables represent components of the macroscopic polarization of the atomic medium:

$$\begin{aligned} \vec{P}(t, z) = & N_c e \text{Tr}[\hat{\rho} \hat{r}] \\ = & N_c [e^{i\omega t - ikz}(\vec{\sigma}^- P_{-+} + \vec{\sigma}^+ P_{++}) \\ & + e^{-i\omega t + ikz}(\vec{\sigma}^- P_{--} + \vec{\sigma}^+ P_{+-})], \end{aligned} \quad (11)$$

where  $N_c$  is the concentration of Rb atoms.

To obtain the angle of rotation  $\phi$  we take the third and fourth lines of equation (8) and set  $\varphi_y = \varphi_x + \frac{\pi}{2}$ :

$$\begin{aligned} E_{++} = & - \frac{(E_x + E_y)}{2\sqrt{2}} e^{i\varphi_x - i\phi}, \\ E_{-+} = & \frac{(E_x - E_y)}{2\sqrt{2}} e^{i\varphi_x + i\phi}, \end{aligned} \quad (12)$$

i.e.,

$$\begin{aligned} |E_{++}| = & \frac{(E_x + E_y)}{2\sqrt{2}}, \quad \arg(E_{++}) = \varphi_x - \phi + \pi + 2\pi n_1, \\ |E_{-+}| = & \frac{(E_x - E_y)}{2\sqrt{2}}, \quad \arg(E_{-+}) = \varphi_x + \phi + 2\pi n_2. \end{aligned} \quad (13)$$

From equation (13) we obtain

$$\phi = \frac{1}{2}(\arg(E_{-+}) - \arg(E_{++}) - 2\pi(n_2 - n_1) + \pi). \quad (14)$$

For the results presented in the next section we have  $\phi(0, 0) = 0$  and from equation (14) we calculate the polarization rotation along the atomic medium and for different times during the pulse propagation  $\phi(t, z)$ .

Results for the transmission of the laser will also be presented in the next section. They represent the power average of the laser electromagnetic field,  $I = c\epsilon_0 \langle \vec{E} \cdot \vec{E} \rangle$ . From equation (7) we have

$$\begin{aligned} I = & c\epsilon_0 \langle \{\vec{\sigma}^- (E_{-+} e^{i\omega t - ikz} + E_{--} e^{-i\omega t + ikz}) \\ & + \vec{\sigma}^+ (E_{++} e^{i\omega t - ikz} + E_{+-} e^{-i\omega t + ikz})\}^2 \rangle \\ = & -2c\epsilon_0 (E_{++} E_{--} + E_{-+} E_{+-}). \end{aligned} \quad (15)$$

### 3. Results and discussion

In this section we present results for the evolution of the NMOR for the linearly polarized light pulse as the pulse propagates through the  $L = 0.1$  m long Rb atomic cloud. The pulse laser frequency is tuned to the  $F_g = 2 \rightarrow F_e = 1$  transition of the  $^{87}\text{Rb}$ , D1 line. Results are calculated for magnetic fields corresponding to the EIT resonance. The spontaneous emission rate is  $\Gamma = 2\pi \cdot 5.75006$  MHz and the concentration of Rb atoms, if not emphasized differently, is  $N_c = 10^{14} \times 1 \text{ m}^{-3}$ . The rate of relaxation due to time of flight  $\gamma = 0.001 \Gamma$ . Temporal wave-form of the propagating laser pulse is Gaussian (see figure 2):

$$I(t) = I^0 \exp\left(-\frac{(t - t_c)^2}{\frac{\Delta_w^2}{4 \log(2)}}\right), \quad (16)$$

where  $I^0$  is the pulse peak intensity at the centre of the pulse  $t_c$  and  $\Delta_w$  is the full-width at half-maximum. We point out that transmission and NMOR signals can readily be obtained experimentally from transient wave-forms of a transmitted laser pulse, at large number of magnetic field values within the EIT spectral bandwidth.

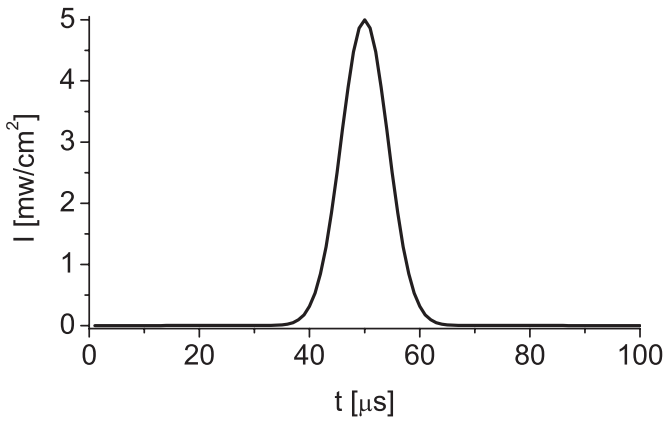


**Figure 2.** Gaussian wave-form of the light pulse used in the calculations. The pulse peak intensity is  $I^0 = 5 \text{ mW cm}^{-2}$ , centred at  $t_c = 50 \text{ } \mu\text{s}$  and  $\Delta_W = 10 \text{ } \mu\text{s}$ .

The origin of EIT lies in the CPT i.e. the existence of a so-called dark state which represents coherent superposition among the ground-state Zeeman sublevels. Mathematically, the dark state is given with the condition  $\hat{H}_I |\text{dark state}\rangle = 0$ . For the scheme  $F_g = 2 \rightarrow F_e = 1$  (see figure 1) there are two dark states, one among  $|m_g = -1\rangle$  and  $|m_g = +1\rangle$  Zeeman sublevels, thus induced by the  $\Lambda$  interacting scheme. The other dark state represents linear combination of other ground-state sublevels, being part of the  $M$  scheme. Due to the existence of these dark states, EIT resonances are closely related to the ground-state Zeeman sublevels and the coherences created between them. Formation of coherences, dark states and optical pumping processes for different CPT schemes among the Zeeman sublevels was analysed by Renzoni *et al* [18] for the sodium D1 line. The role of ground-state coherences in the NMOR effect was also discussed [19, 20]. Matsko *et al* [19] analysed ellipticity-dependent nonlinear magneto-optic rotation of elliptically polarized light propagating in a medium with atomic coherence. It was shown that this rotation can be described by means of  $\Lambda$ ,  $M$  and higher-chain  $\Lambda$  schemes. Drampyan *et al* [20] presented a theoretical description based on the inverted Y model (combination of the  $\Lambda$  and ladder systems).

In figure 3 we compare behaviour of the pulse transmission and the rotation angle  $\phi$  versus the magnetic field  $B$  with the behaviour of the ground-state coherence  $\rho_{g-1,g1}$ . We present results for three moments of the pulse propagation corresponding to different intensities of the pulse in the medium: during rising of the pulse intensity ((a) and (d)), when the pulse is at the maximum intensity ((b) and (e)) and during falling of the pulse intensity ((c) and (f)). More precisely, these three instances correspond to times  $t = 40 \text{ } \mu\text{s}$ ,  $t = 50 \text{ } \mu\text{s}$  and  $t = 64 \text{ } \mu\text{s}$  of the linearly polarized Gaussian pulse presented in figure 2. Results presented in figures 3(a)–(c) show that evolution of both EIT and NMOR show various dependences on  $B$  while the pulse intensity varies. Both magnitude of the polarization rotation angle and the shape of its dependence on  $B$  is very sensitive on the pulse intensity in the medium. There are also significant differences of both EIT and NMOR depending on whether the pulse intensity is rising or falling. Results for the dependence of the NMOR on  $B$  in figure 3(c),

calculated for the time when the pulse is ‘leaving’ the medium,  $t = 64 \text{ } \mu\text{s}$ , show oscillatory behaviour of rotation angle  $\phi$ , that can be related to the Ramsey effect. Polarization of atoms created at the peak of the pulse is probed during the weaker pulse intensity at the time when the pulse exits the medium [21, 22]. For the same moments of the pulse propagation, results for the behaviour of the ground-state coherence  $\rho_{g-1,g1}$ , presented in figures 3(d)–(f) reveal a close relation between transmission of the pulse and the real part of  $\rho_{g-1,g1}$ , and between the dispersive shape of the rotation angle and the imaginary part of  $\rho_{g-1,g1}$ .

To further confirm the relation between NMOR and ground-state coherences, in figure 4 we compare amplitudes (a) and widths (b) of the angle of rotation  $\phi$  (green curves) and of the imaginary part of  $\rho_{g-1,g1}$  (blue curves) as a function of the magnetic field  $B$ , for different times during the pulse propagates through the medium. Amplitudes and widths were obtained from dispersively shaped dependence on  $B$  (green and blue curves in figure 3) i.e. from their minimum ( $B < 0$ ) and maximum ( $B > 0$ ) values. The NMOR amplitude represents the difference between these two extreme values of the rotation angle, while the NMOR width is the difference between the corresponding values of the magnetic field. Widths and amplitudes of the magnetic field dependence of  $\rho_{g-1,g1}$  are calculated in an analogous way. Results show that the transient behaviour of the amplitudes and widths of NMOR and the imaginary part of coherence  $\rho_{g-1,g1}$  closely follow each other. Discrepancy between widths at the time when the pulse begins to enter the medium is due to the fact that formation of NMOR signal is slower than the coherence buildup.

Results presented in figure 4 reflect diversity of the magnetic field dependence of rotation angle  $\phi(B)$  during pulse propagation through the medium of Rb atoms. During the rising of the pulse intensity, when the pulse starts to enter the medium, there is a linear-like dependence of the NMOR amplitude with increasing intensity. With rising of the pulse intensity, atoms are exposed to larger energy per unit surface area, as given with the integral of the pulse intensity over time i.e. the area of the pulse. Results presented in figure 4(a) show the effect of saturation at around  $t = 43 \text{ } \mu\text{s}$ , that is before the pulse peak intensity enters the medium. Further increase of the intensity leads to smaller amplitudes of  $\phi(B)$  at the pulse peak intensity. Results in figure 4 show that, for times when pulse intensity is falling, the resonances are becoming steeper i.e. the width of  $\phi(B)$  is decreasing and amplitude is becoming larger.

Next, we analyse the effect of the pulse peak intensity and width on the behaviour of NMOR. In figure 5(a) we present the amplitude of  $\phi(B)$  versus time for three light pulses of the same width  $\Delta_W = 10 \text{ } \mu\text{s}$ , centred at  $t_c = 50 \text{ } \mu\text{s}$  and with different peak intensities  $I^0 = 0.1 \text{ mW cm}^{-2}$  (magenta curve),  $I^0 = 0.5 \text{ mW cm}^{-2}$  (green curve) and  $I^0 = 1 \text{ mW cm}^{-2}$  (black curve). In figure 5(b) the NMOR amplitude is presented for three pulses with peak intensity  $I^0 = 0.3 \text{ mW cm}^{-2}$  and different widths,  $\Delta_W = 10 \text{ } \mu\text{s}$  (magenta curve),  $\Delta_W = 20 \text{ } \mu\text{s}$  (green curve) and  $\Delta_W = 40 \text{ } \mu\text{s}$  (black curve). For results presented in figure 5(b), the pulses were centred at  $t_c = 100 \text{ } \mu\text{s}$  to ensure that for  $t = 0$  pulse intensity represents numerical zero.

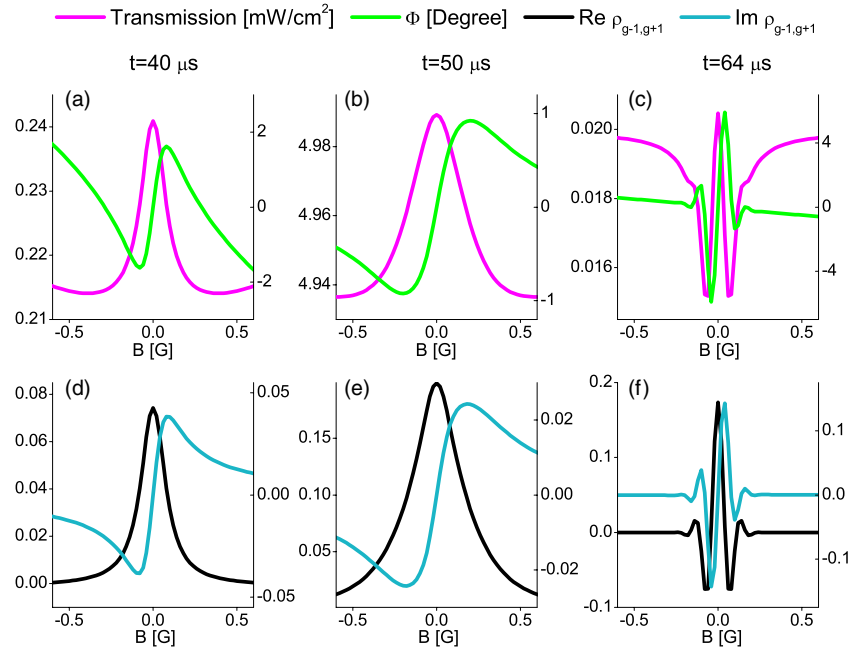


**Figure 3.** Results for the magnetic field dependence of transmission (magenta curves), rotation angle  $\phi$  (green curves) and imaginary (blue curves) and real (black curves) parts of the ground-state coherence  $\rho_{g-1,g+1}$  for three different moments of the pulse propagation:  $t = 40 \mu s$  ((a) and (d)),  $t = 50 \mu s$  ((b) and (e)) and  $t = 64 \mu s$  ((c) and (f)). Results are presented for the linearly polarized pulse with the peak intensity  $I^0 = 5 \text{ mW cm}^{-2}$ ,  $t_c = 50 \mu s$  and  $\Delta_W = 10 \mu s$  shown in figure 2. y-scales for the rotation angle and the imaginary part of  $\rho_{g-1,g+1}$  are given on the right sides.

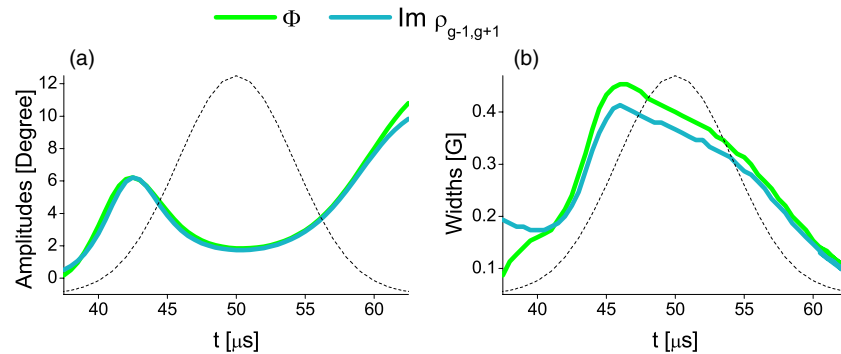


**Figure 4.** Results for amplitude (a) and width (b) of NMOR (green curves) and imaginary part of the ground-state coherence  $\rho_{g-1,g+1}$  (blue curves) during the light pulse passing through the medium. Results for the amplitude of the imaginary part of coherence were multiplied with the constant to coincide with amplitudes of  $\phi(B)$ . Also presented with black dashed lines are normalized wave-forms of the pulse. Parameters are the same as in figure 3.

The effect of the pulse peak intensity and width on the NMOR has to be related to the light absorbed by the atomic medium since the beginning of the interaction of the atomic ensemble with the light pulses. Dependences of amplitudes with the time of the pulse propagation, presented in figure 5, show their increase when pulse intensity is rising. However, while the magenta curves in both figures 5(a) and (b) constantly increase even when the pulse is leaving the medium, the results for higher pulse peak intensities and larger pulse width show that there are critical moments when the amplitude of the  $\phi(B)$  starts to decrease. This results in smaller polarization rotation although the pulse intensity is rising. Exposing the atoms to higher pulse energy, either by the increase of the pulse peak intensity or with wider  $\Delta_W$ , leads to saturation and even decrease of NMOR amplitudes during high pulse intensities.

This effect is relaxed with the lower intensity when the pulse is leaving the medium, leading to even higher amplitudes than for pulse intensities during the rising side of the pulse. This kind of dependence of the NMOR amplitude with time is characteristic for much larger intensities, as presented in figure 4.

Our analysis shows that a decrease of polarization rotation, while pulse intensity is still increasing, is related to the optical pumping into the dark state. Here we analyse the dark state formed only by the  $\Lambda$  scheme, while the analysis of the other dark state ( $M$ -scheme) brings very similar results. In figure 6(a) we present results for the behaviour of the population of the dark state as a function of time for three values of the magnetic fields  $B = 0$  (magenta curves),  $B = 0.1 \text{ G}$  (green curves) and  $B = 0.2 \text{ G}$  (black curves). Presented in figure 6(b) is the imaginary part of the

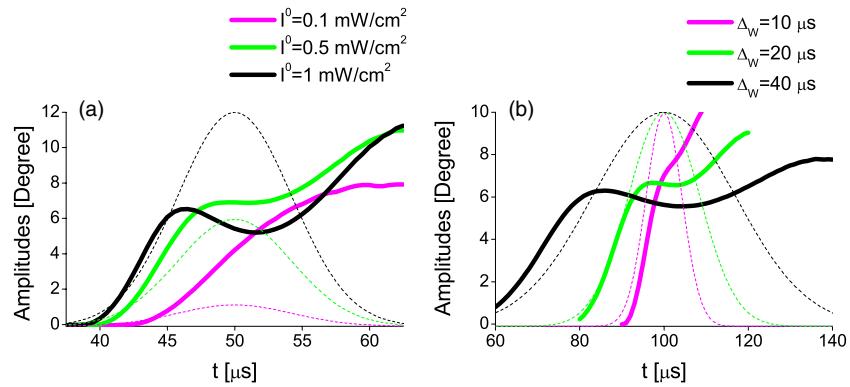


**Figure 5.** NMOR amplitudes at different times during the light pulse propagation through the medium. In (a) we present results for the pulse with  $\Delta_W = 10 \mu\text{s}$ ,  $t_c = 50 \mu\text{s}$  and for three different pulse peak intensities:  $I^0 = 0.1 \text{ mW cm}^{-2}$  (magenta curve),  $I^0 = 0.5 \text{ mW cm}^{-2}$  (green curve) and  $I^0 = 1 \text{ mW cm}^{-2}$  (black curve). In (b) we present results for the pulse with  $I^0 = 0.3 \text{ mW cm}^{-2}$ ,  $t_c = 100 \mu\text{s}$  and for three different widths of the pulse:  $\Delta_W = 10 \mu\text{s}$  (magenta curve),  $\Delta_W = 20 \mu\text{s}$  (green curve) and  $\Delta_W = 40 \mu\text{s}$  (black curve). Also presented with dashed lines of matching colours are the wave-forms of the corresponding light pulses.

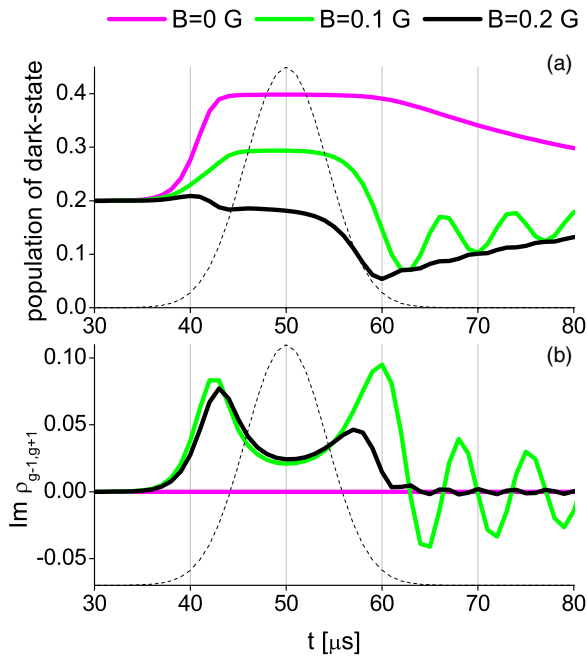


**Figure 6.** Time-dependence of the population of the  $\Lambda$ -scheme dark state (a) and imaginary part of the ground-state coherence  $\rho_{g-1,g+1}$  (b) for three magnetic fields:  $B = 0 \text{ G}$  (magenta curves),  $B = 0.1 \text{ G}$  (green curves) and  $B = 0.2 \text{ G}$  (black curves). Results are for the linearly polarized pulse presented in figure 2:  $I^0 = 5 \text{ mW cm}^{-2}$ , centred at  $t_c = 50 \mu\text{s}$  and  $\Delta_W = 10 \mu\text{s}$ . Normalized wave-forms of the pulse are presented with black dashed lines.

coherence  $\rho_{g-1,g+1}$ , which constitutes the dark state from the  $\Lambda$ -scheme. Results are for the linearly polarized pulse presented in figure 2.

For the considered configuration, the condition for the dark state is satisfied only for the zero magnetic field, while for other magnetic fields, inside the EIT resonance, the EIT profile represents the ‘grey zone’ where the absorption is less suppressed. Results in figure 6(a) show that for  $B = 0$  the population of the dark state is constantly trapped during most of the time of the pulse propagation, while the non-zero magnetic fields yield a less populated dark state. For non-zero

magnetic fields and times when the population of the dark state shows a flat dependence of maximally trapped atoms in the dark state, the magnitude of the imaginary part of the coherence  $\rho_{g-1,g+1}$ , decreases during the rising of the pulse intensity, and recovers after the pulse peak intensity. Maximally populated dark states lead to suppressed absorption which in turn leads to depolarization of atoms and less rotation. The decrease of  $\phi(B)$  amplitudes during the pulse maximum intensity is the result of optical pumping into the dark states, followed by simultaneous decrease of coherences with time, but also dependent on the value of the magnetic field  $B$ .

The subject of many studies is the width of EIT [18, 23–26]. Being both related to the ground-state coherences, EIT and NMOR also depend on the lifetimes of ground-state coherences created between ground-state Zeeman sublevels. In our model, we have taken into account relaxation of all density matrix elements with rate  $\gamma$ , due to the finite time that atoms spend in the laser beam. While the lifetimes of excited state and optical coherences are limited by the spontaneous emission rates, the lifetime of the ground-states is much longer and is determined with  $\gamma$ .

In figure 7 we present dependences of the NMOR amplitude (a) and the NMOR width (b) on the time-dependent intensity of the linearly polarized laser pulse (shown in figure 2) for three values of relaxation rates:  $\gamma = 0.0001 \Gamma$  (magenta curve),  $\gamma = 0.001 \Gamma$  (green curve) and  $\gamma = 0.01 \Gamma$  (black curve). The presented results show that the value of the relaxation rate  $\gamma = 0.01 \Gamma$  (black curves in figure 7) yields qualitatively and quantitatively different behaviour of both NMOR amplitude and width, compared to the smaller relaxation rates. During rising of the pulse intensity, while the dark states are not yet populated, the influence of large  $\gamma$  means greater dissipation of the ground-state populations and the coherences and thus slower formation of the dark states. For times when saturation of NMOR is present, the rate of relaxation of the ground-states strongly influences the widths of the rotation angles. The width of  $\phi(B)$  for  $\gamma = 0.01 \Gamma$  (black curve in figure 7(b)) is significantly larger compared to the results with smaller  $\gamma$ . Also, the black curve in figure 7(a) shows a decrease of the amplitude when the pulse

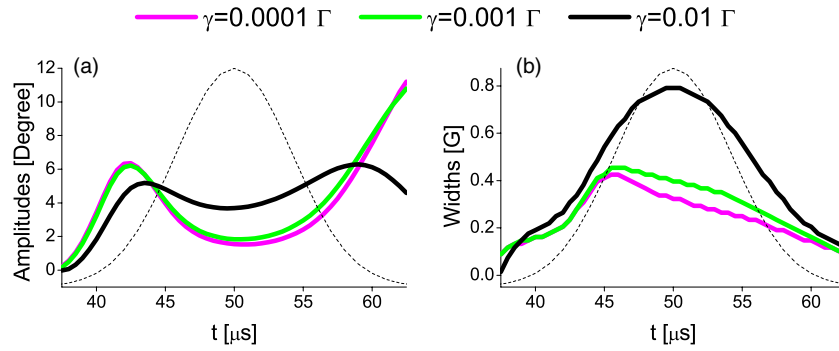


**Figure 7.** Time-dependence of the amplitude (a) and the width (b) of  $\phi(B)$ , for the ground-state relaxation rates:  $\gamma = 0.0001 \Gamma$  (magenta curve),  $\gamma = 0.001 \Gamma$  (green curve) and  $\gamma = 0.01 \Gamma$  (black curve). Results are for the linearly polarized pulse and the peak intensity is  $I^0 = 5 \text{ mW cm}^{-2}$ , centred at  $t_c = 50 \mu\text{s}$  and with the  $\Delta_W = 10 \mu\text{s}$ , presented in figure 2. Normalized wave-forms of the pulse are presented with black dashed lines.

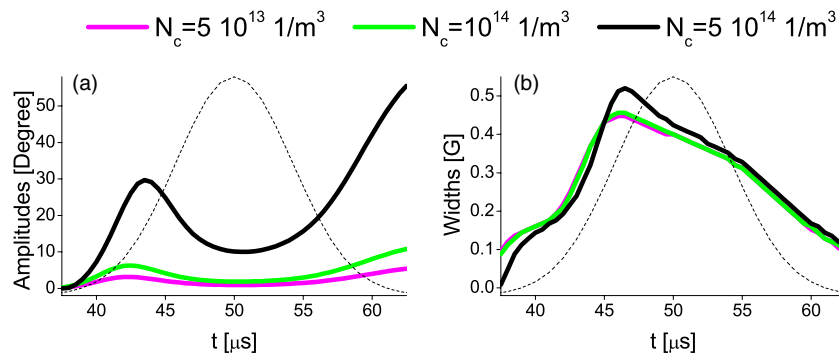


**Figure 8.** Dependence of the amplitude (a) and the width (b) of the  $\phi(B)$  on the time of pulse propagation for three different concentrations of Rb atoms in the medium:  $N_c = 5 \times 10^{13} \times 1 \text{ m}^{-3}$  (magenta curves),  $N_c = 10^{14} \times 1 \text{ m}^{-3}$  (green curves) and  $N_c = 5 \times 10^{14} \times 1 \text{ m}^{-3}$  (black curves). Results are presented for the linearly polarized pulse with the peak intensity  $I^0 = 5 \text{ mW cm}^{-2}$ ,  $t_c = 50 \mu\text{s}$  and  $\Delta_W = 10 \mu\text{s}$  as shown in figure 2. Normalized pulse wave-forms are presented with black dashed lines.

is leaving the medium. During this period, intensities of the pulse are insufficient to sustain created coherences due to great dissipation with the rate  $\gamma = 0.01 \Gamma$ . Effect of decoherence on the NMOR was previously studied by Wang *et al* [27]. It was pointed out that an increase of decoherence rate leads to the behaviour typical for a linear Faraday rotator because the EIT effect tends to be eliminated. The shift of the peak of the Faraday rotation angle to higher magnetic fields was observed [27], which can be related to an increased width of  $\phi(B)$  in our analysis for the case of pulsed light.

Results presented in figure 8 demonstrate the influence of the optical thickness of the atomic gas on the NMOR. We present results for the amplitude (a) and width (b) of the calculated  $\phi(B)$  as a function of time-dependent laser intensity. Results are for the linearly polarized pulse presented in figure 2. Calculations were performed for three values of the atomic density  $N_c = 5 \times 10^{13} \times 1 \text{ m}^{-3}$  (magenta curves),  $N_c = 10^{14} \times 1 \text{ m}^{-3}$  (green curves) and  $N_c = 5 \times 10^{14} \times 1 \text{ m}^{-3}$  (black curves). Results presented in figure 8 show that atomic density does not influence the width of NMOR significantly. Conversely, amplitudes are strongly affected with the change of atomic density yielding approximately an order of magnitude greater rotation when the concentration is changed by an order of magnitude. The effect of the atomic density in our theoretical model is in the macroscopic polarization of atomic medium (see equation (11)), which depends linearly

on the atomic concentration. Atomic concentration determines the number of polarized atoms whose atomic polarization is precessing in the magnetic field, and therefore changes the properties of the optical medium. The change of atomic density also strongly affects polarization of the pulse itself, since components of the atomic polarization are in the right-hand sides of equation (9) and represent source terms of the Maxwell–Bloch equations. The effect of atomic density on the nonlinear Faraday effect with intense linearly polarized light in an optically thick atomic rubidium vapour was previously studied by Hsu *et al* [28] for the CW field. They show that the polarization rotation rate, which is rotation angle per unit magnetic field  $d\phi/dB$ , in the limit of low field has a maximum value as the density is increased.

#### 4. Conclusions

We analysed NMOR of the linearly polarized Gaussian pulse while propagating through the cold atomic gas. The frequency of the laser pulse is tuned to the  $F_g = 2 \rightarrow F_e = 1$  transition in  $^{87}\text{Rb}$ , D1 line, and the pulse induces EIT. Transient non-monotonic dependence of the rotation angle is obtained, with enhancement and suppression of magneto-optical rotation during different phases of the pulse propagation. Throughout the pulse propagation, NMOR (EIT) behaves similarly to the imaginary (real) part of the ground-state Zeeman coherences.

NMOR depends on optical pumping into the dark states and on the behaviour of ground-state coherences subjected to CPT. Behaviour of pulse NMOR qualitatively changes for different values of the pulse peak intensity. For the pulse with peak intensity of  $I^0 = 5 \text{ mW cm}^{-2}$ , the initial increase of the NMOR is followed by the decrease when the pulse intensity increases and nears its peak value. For pulses of much smaller peak intensity, the magnitude of NMOR increases all the time during the pulse propagation. It was shown that the relaxation of the ground-states affects the width of the dispersive-shaped magnetic field dependence of polarization rotation angle—the maximum of NMOR shifts to higher magnetic field as the relaxation increases. Our results have shown the effect of the density of Rb atoms, i.e., for the range of considered parameters, the magnitude of the NMOR scales nearly linearly with the concentration of atoms. Results presented in this paper are of interest in all studies of the propagation of a Gaussian pulse through the media under the conditions of EIT and in the presence of external magnetic field.

### Acknowledgment

This work was supported by the Ministry of Education, Science and Technological Development of the Republic of Serbia, under grants number III 45016 and OI 171038.

### References

- [1] Budker D, Gawlik W, Kimball D F, Rochester S M, Yashchuk V V and Weis A 2002 *Rev. Mod. Phys.* **74** 1153
- [2] Alexandrov E B, Auzinsh M, Budker D, Kimball D F, Rochester S M and Yashchuk V V 2005 *J. Opt. Soc. Am. B* **22** 7
- [3] Sautenkov V A, Lukin M D, Bednar C J, Novikova I, Mikhailov E, Fleischhauer M, Velichansky V L, Welch G R and Scully M O 2000 *Phys. Rev. A* **62** 023810
- [4] Akhmedzhanov R A and Zelensky I V 2002 *JETP Lett.* **76** 419
- [5] Pandey K, Wasan A and Natarajan V 2008 *J. Phys. B: At. Mol. Opt. Phys.* **41** 225503
- [6] Harris S E 1997 *Phys. Today* **50** 369
- [7] Fleischhauer M, Imamoglu A and Marangos J P 2005 *Rev. Mod. Phys.* **77** 633
- [8] Alzetta G, Gozzini A, Moi L and Orriols G 1976 *Nuovo Cimento B* **36** 5
- [9] Arimondo E 1996 *Prog. Opt.* **35** 257
- [10] Harris S E, Field J E and Kasapi A 1992 *Phys. Rev. A* **46** R29
- [11] Kasapi A, Jain M, Yin G Y and Harris S E 1995 *Phys. Rev. Lett.* **74** 2447
- [12] Lezama A, Akulshin A M, Sidorov A I and Hannaford P 2006 *Phys. Rev. A* **73** 033806
- [13] Wang K, Peng F and Yang G 2003 *J. Opt. B: Quantum Semiclass. Opt.* **5** 44
- [14] Qi Y, Niu Y, Zhou F, Peng Y and Gong S 2011 *J. Phys. B: At. Mol. Opt. Phys.* **44** 085502
- [15] Budker D, Kimball D F, Rochester S M and Yashchuk V V 1999 *Phys. Rev. Lett.* **83** 1767
- [16] Gao H, Rosenberry M, Wang J and Batelaan H 2005 *J. Phys. B: At. Mol. Opt. Phys.* **38** 1857
- [17] Ruseckas J, Juzelinis G, Ohberg P and Barnett S M 2007 *Phys. Rev. A* **76** 053822
- [18] Renzoni F, Maichen W, Windholz L and Arimondo E 1997 *Phys. Rev. A* **55** 3710
- [19] Matsko A B, Novikova I, Zubairy M S and Welch G R 2003 *Phys. Rev. A* **67** 043805
- [20] Drampyan R, Pustelny S and Gawlik W 2009 *Phys. Rev. A* **80** 033815
- [21] Krmpot A J, Ćuk S M, Nikolić S N, Radonjić M, Slavov D G and Jelenković B M 2009 *Opt. Express* **17** 22491
- [22] Ćuk S M, Radonjić M, Krmpot A J, Nikolić S N, Grujić Z D and Jelenković B M 2010 *Phys. Rev. A* **82** 063802
- [23] Ye C Y and Zibrov A S 2002 *Phys. Rev. A* **65** 023806
- [24] Figueroa E, Vewinger F, Appel J and Lvovsky A I 2006 *Opt. Lett.* **31** 2625
- [25] Strekalov D, Matsko A B and Maleki L 2005 *J. Opt. Soc. Am. B* **22** 65
- [26] Pack M V, Camacho R M and Howell J C 2007 *Phys. Rev. A* **76** 013801
- [27] Wang J 2010 *Phys. Rev. A* **81** 033841
- [28] Hsu P S, Patnaik A K and Welch George R 2008 *Phys. Rev. A* **78** 053817